THE JOURNAL OF PHYSICAL CHEMISTRY B

Article

pubs.acs.org/JPCB

# Investigation on the Structure of Water/AOT/IPM/Alcohols Reverse Micelles by Conductivity, Dynamic Light Scattering, and Small Angle X-ray Scattering

Xiaoguang Zhang,*[,†] Yingjun Chen,[†] Jiexiang Liu,*[,‡] Chuanzhuang Zhao,[†] and Haijiao Zhang[‡]

[†]College of Chemistry, Nankai University, Tianjin 300071, People's Republic of China

[‡]School of Chemical Engineering, Hebei University of Technology, Tianjin 300130, People's Republic of China

Supporting Information

**ABSTRACT:** We have systematically investigated the effect of alcohols (ethanol, propanol, butanol, and pentanol) on the structure of the water/AOT/IPM system using conductivity, dynamic light scattering (DLS), and small-angle X-ray scattering (SAXS) techniques. The results show that no percolation phenomenon is observed in the water/AOT/IPM system, whereas the addition of ethanol (propanol and butanol) induces apparently percolation. The threshold water content ($W_p$) depends closely on the alcohol type and concentration. The effect of alcohols on the conductance behavior is discussed from the physical properties of alcohols, the interfacial flexibility, and the attractive interactions between droplets. The hydrodynamic diameter of droplets ($d_H$) obtained from DLS increases markedly with the increase in water content ($W_0$); however, it decreases gradually with increasing alcohol chain length and concentration. SAXS measurements display distinctly the shoulder, the low hump peaks, and the heavy tail phenomenon in the pair distance distribution function $p(r)$ profile, which rely strongly on the alcohol species and its concentration. The gyration radius ($R_g$) increases with increasing $W_0$, and decreases with the increase of alcohol chain length and concentration. Schematic diagram of the conductance mechanism of water/AOT/IPM/alcohol systems is primarily depicted. Three different phases of the discrete droplets, the oligomers, and the isolated ellipsoidal droplets existed in the different $W_0$ ranges correspond to three different stages in the conductivity−$W_0$ curve. Coupling the structure characteristics of reverse micelles obtained from DLS and SAXS techniques with conductivity could be greatly helpful to deeply understand the percolation mechanism of water/AOT/IPM/alcohols systems.

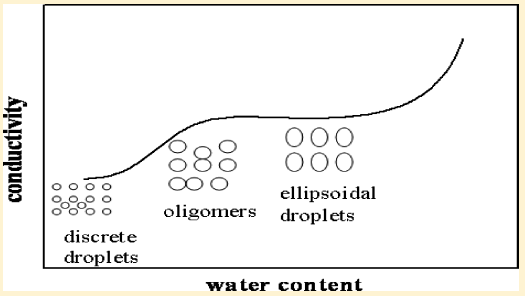


## 1. INTRODUCTION

Reverse micelles (reverse microemulsions) are thermodynamically stable and isotropic systems that are constituted by water, oil, and one or more surfactants. The structure and properties of reverse micelles have been extensively investigated by employing a variety of physicochemical techniques, such as FT-IR,[1,2] NMR,[3] fluorescence spectroscopy,[4,5] conductivity,[6,7] calorimetry,[8,9] dynamic light scattering (DLS),[10−12] and small-angle X-ray scattering (SAXS),[13−15] etc. Of these, the conductivity method provides a particularly convenient, useful, and accessible tool for probing the structure and phase behaviors of reverse microemulsions.[16,17] Percolation of conductance is one of the important physicochemical properties of w/o microemulsions, and it is generally believed that during the percolation process dispersed water droplets cluster/associate and ions either "hop"[18] from droplet to droplet or are transferred by way of "transient fusion and mass exchange".[19] In addition, the DLS technique is relatively easy to perform and useful to measure particle size distribution; however, it is difficult to extract information about geometrical features such as shape and stability. Furthermore, SAXS is a widely used technique for the direct structural investigations of the systems with the inner structuration falling in the colloidal domain. In recent years, DLS and SAXS techniques have already been combined to comprehensively understand the structure of microemulsion.[20−23] In the present study, the combination of DLS and SAXS techniques is employed and provides better insight into micelles by probing the structure of water/AOT/IPM/alcohol systems.

A common surfactant used to form reverse micelles is bis(2-ethylhexyl) sulfosuccinate sodium salt (AOT) because the micelles formed with this surfactant can solubilize a large quantity of water in a nonpolar solvent.[24,25] Over the past decades, many studies have focused on the effect of various additives (organic substances, electrolytes, cosurfactants, and nonionic surfactants) on conductivity behavior of water/AOT/alkane systems, and some mechanisms for these effects have been put forward.[26−30] Compared to alkane, isopropyl myristate (IPM) is a kind of nontoxic lipophilic oil, which has been widely used in biologically resembling systems, and

Received: November 12, 2011
Revised: February 7, 2012
Published: March 1, 2012

pharmaceutical and drug delivery systems.[31,32] Mitra and Paul have detailed investigated solubilization and conductance behaviors of water/AOT/nonionic surfactants/IPM systems.[33−36] They have found that water/AOT/Brij-52 (or Spans) /IPM systems do not exhibit the percolation phenomenon, whereas temperature-induced percolation is detected by adding Brij-35, Brij-56, Brij-58, Brij-76, Tween-20, Tween-40, and Igepal CO 520. Furthermore, the addition of Brij-56 and Brij-58 induces water-induced percolation, respectively. The threshold water content and temperature depend on the type, headgroup configuration, and content of nonionic surfactants. It is often necessary to add a cosurfactant, typically a medium chain length alcohol, to water, oil, and surfactant to form a microemulsion. Different researchers have carried out extensive studies to understand the effect of alcohols on the physicochemical properties of microemulsion.[3,37−42] Also, there have been a few studies on microemulsions with IPM/alcohol as oil phase,[3,31,40,43] but the role of alcohol remains unclear. The effect of alcohol on the solubilization and microstructure of water/AOT/IPM/alcohol system is still unclear. This motivates us to carry out a comprehensive investigation of water/AOT/IPM/alcohol systems, which benefits understanding completely the percolation mechanism of microemulsions based on IPM.

In the present paper, we have investigated systematically the effect of water content, alcohol type, and its concentration on the conductance behaviors of water/AOT/IPM/alcohol systems. Besides, our study focuses primarily on coupling DLS with SAXS techniques to gain better insight on the morphological and size aspects of reverse micelles, and to further understand the percolation mechanism of water/AOT/IPM/alcohol systems.

## 2. EXPERIMENTAL SECTION

**2.1. Materials.** AOT (99% pure) purchased from Sigma, USA, dried at 60 °C for 48 h in a vacuum, stored over $P_2O_5$ in a desiccator, and used without further purification. Ethanol, propanol, butanol, and pentanol (A.R. grade) were purchased from North Tianjin Pharmacy Chemical Reagent Co. and stored over 4A molecular sieves before use. IPM was purchased from Sinopharm Chemical Reagent Co. Ltd. and was stored over anhydrous $MgSO_4$ after decompression distillation before use. All the aqueous solutions were prepared in doubly distilled water with conductivity 2−4 $\mu$S cm$^{-1}$ at 30 °C.

**2.2. Electrical Conductance, Water Solubilization Capacity, and Viscosity.** The oil phase of 0.1 mol·L$^{-1}$ AOT in IPM or IPM/alcohol was prepared at ambient temperature. The alcohol concentration ($\nu$(alcohol)) is the volume fraction of alcohol in the mixed solvents of IPM and alcohol. The conductivity ($\sigma$) of microemulsion was measured by using a DDSJ-308A digital conductometer (Shanghai Precision & Scientific Instrument Co. Ltd., China). The dependence of conductivity on water content was carried out as water was gradually injected into the oil phase under stirring at (30.0 ± 0.1) °C, and water content ($W_0$) was expressed as the molar ratio of water to AOT. The water solubilization capacity was determined by visual observation of phase separation in the course of the conductivity measurements, which corresponded to the maximal $W_0$ value in the curve of $\sigma$ versus $W_0$. The turbidity of the system often increased greatly before phase separation, and the last additions were performed more slowly. The viscosity of IPM/alcohol was measured by RS600 rheology (Thermo Electron Corp., USA) at (30.0 ± 0.1) °C.

**2.3. Dynamic Light Scattering Measurements.** Dynamic light scattering measurements were performed using Zeta PALS + BI-90 plus (Brookhaven Co., USA) fitted with a 30 mW laser, operating at 659 nm, and placing the sample tube in the thermostated chamber. All measurements were taken at 90°. Each sample was filtered through a Millipore 0.20 $\mu$m membrane filter prior to taking measurement. The DLS intensity data were processed using the CONTIN software to obtain the diffusion coefficient ($D$), and hydrodynamic diameter ($d_H$) of the samples. DLS measurements were taken at (30.0 ± 0.1)°C.

**2.4. Small-Angle Scattering Measurements and Data Analyses.** The size and shape of droplets in reverse microemulsion were evaluated by small-angle X-ray scattering measurements. SAXS experiments were carried out by using a Bruker Nanostar (Bruker AXS, Germany) with a 2D detector (Bruker Histar), and were operated at 40 kV and 35 mA. The wavelength of the incident X-ray beam from Cu K$\alpha$ radiation was $\lambda$ = 0.154 nm. The distance from the sample to the detector was selected approximately 67 cm for low $W_0$ and 108 cm for high $W_0$, which was calibrated by silver behenate. The sample was sealed in a 1.0 mm quartz capillary tube, and all measurements were performed at (28 ± 1) °C. The scattering from IPM (IPM/alcohol mixed solvents) was subtracted as background from that of the reverse microemulsion.

Data was analyzed in the indirect transformation procedure of Glatter.[44] The pair distance distribution function $p(r)$ was obtained by Fourier transform of the scattering intensity $I(q)$ as

$$p(r) = \frac{1}{2\pi^2}\int_0^\infty rqI(q)\sin(rq)\,dq \tag{1}$$

$$q = (4\pi/\lambda)\sin(\theta/2) \tag{2}$$

where $q$ is the amplitude of the scattering vector, $\theta$ and $\lambda$ are the scattering angle and the X-ray wavelength, and $r$ is a distance in real space. The expression gives the frequency of occurrence of vector of length $r$, weighted by the electron density at either end of the vector. The $p(r)$ function depends both on the particle geometry and on the inner heterogeneity of the scattering density distribution in the particle. The gyration radius of particles ($R_g$) was determined by using the following equation

$$R_g^2 = \frac{\int_0^{D_{max}} p(r)r^2\,dr}{2\int_0^{D_{max}} p(r)\,dr} \tag{3}$$

where $D_{max}$ is the maximum diameter of the particle and is estimated from the $p(r)$ function satisfying the condition $p(r)$ = 0 for $r > D_{max}$. The shape of the $p(r)$ curve directly reflects the form of the microemulsion droplets for a monodisperse population.

## 3. RESULTS AND DISCUSSION

**3.1. Conductance Behavior of Water/AOT/IPM/Alcohol Systems.** Dependence of $\sigma$ on $W_0$ in water/AOT/IPM system is first measured and represented in Figure S1 of the Supporting Information. Reverse micelles formed by AOT in IPM oil can solubilize water up to $W_{0,max} \approx 24$. As $W_0 \leq 2$, $\sigma$ is smaller than 0.01 $\mu$S·cm$^{-1}$ that goes beyond the detection limit of the apparatus; then $\sigma$ increases with increasing $W_0$, followed


dx.doi.org/10.1021/jp210902r | J. Phys. Chem. B 2012, 116, 3723−3734

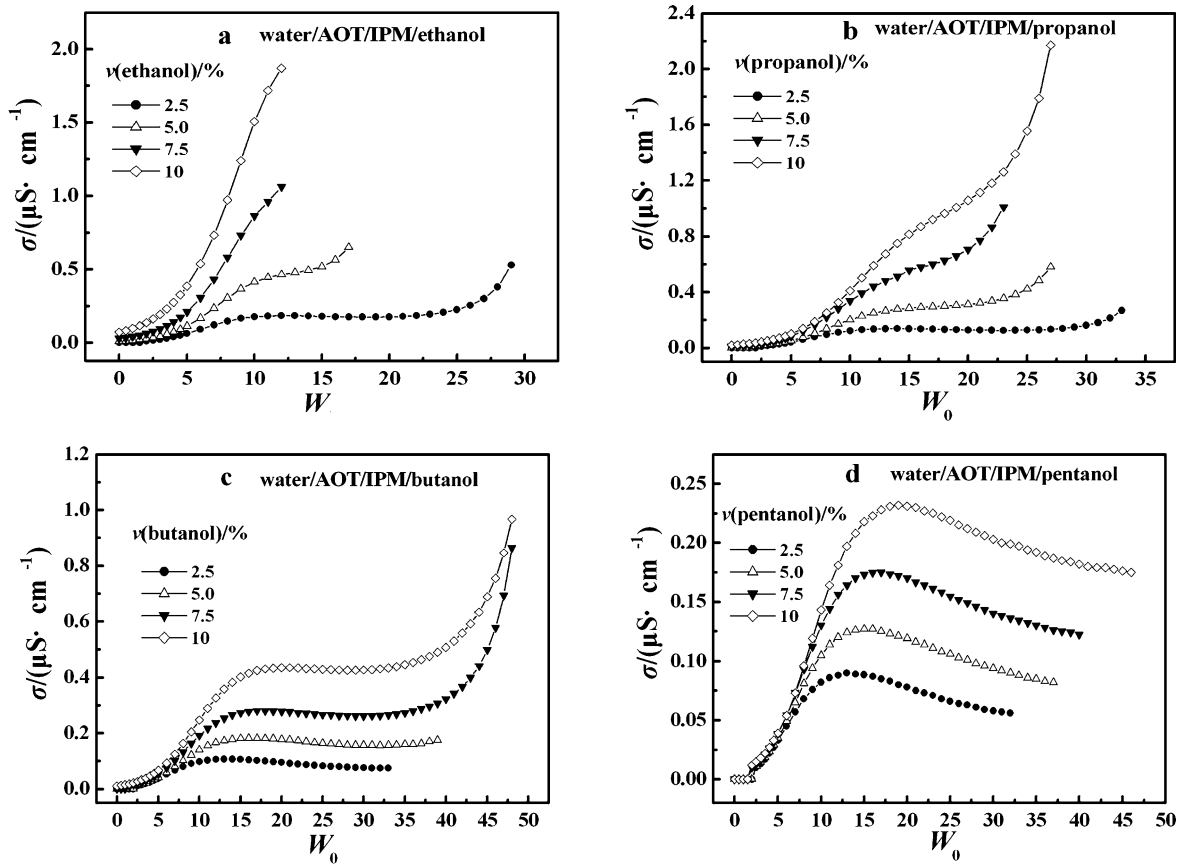


**Figure 1.** Dependence of $\sigma$ on $W_0$ in water/AOT/IPM/alcohol systems with different volume fractions of alcohol.

by a gradual decrease as $W_0 > 12$. No percolation phenomenon is detected in the water/AOT/IPM system. This conductivity behavior has been reported by Mitra et al.,[36] and no percolation may be due to the rigidity of interfacial film, large molar volume, and high viscosity of IPM.

The dependence of $\sigma$ on $W_0$ in water/AOT/IPM/ethanol (propanol, butanol, and pentanol) systems with different alcohol volume fractions is systematically investigated and displayed in Figure 1. Compared to the water/AOT/IPM system, $\sigma$ of water/AOT/IPM/ethanol (propanol, butanol, and pentanol) systems increase evidently with the increase of alcohol concentration from 2.5 to 10%. In Figure 1a, for the water/AOT/IPM/ethanol ($\nu$(ethanol) = 2.5%) system ($\nu$(ethanol) represents volume percent of added ethanol in mixed solvents of IPM and ethanol), the curve of $\sigma$ vs $W_0$ presents three stages: $\sigma$ increases initially until the maximum at $W_0 \leq 10$ (I); then it remains almost constant at $10 < W_0 \leq 23$ (II); and finally it increases drastically at $W_0 > 23$ (III), indicating a conductance percolation occurrence. The curve of the water/AOT/IPM/ethanol ($\nu$(ethanol) = 5.0%) system is on the whole similar to that of the water/AOT/IPM/ethanol ($\nu$(ethanol) = 2.5%) except that the II stage shortens markedly. For water/AOT/IPM/ethanol ($\nu$(ethanol) = 7.5, 10%) systems, $\sigma$ increase slowly with $W_0$ at $W_0 \leq 3$, followed by a sharp increase, and the II stage of the curves disappears instead. It is obvious that ethanol induces percolation. In Figure 1b, the effect of propanol on the percolation resembles basically that of ethanol. However, the dependence of $\sigma$ on $W_0$ in the II stage changes a little with increasing propanol concentration: $\sigma$ decreases slightly with increasing $W_0$ in the water/AOT/IPM/propanol ($\nu$(propanol) = 2.5%) system; it stays almost unchanged in the propanol ($\nu$(propanol) = 5.0%) system; and it increases remarkably in the propanol ($\nu$(propanol) = 7.5, 10%) systems. In Figure 1c, the curves of water/AOT/IPM/butanol ($\nu$(butanol) = 7.5, 10%) systems display obviously the I, II, and III stages; whereas only the I and II stages present apparently in the butanol ($\nu$(butanol) = 2.5, 5.0%) systems. This can be correlated with water solubilization capacity of butanol system. The water solubilization capacity enhances gradually with the increase of butanol content. Additionally, the percolation phenomenon can be clearly observed in water/AOT/IPM/butanol ($\nu$(butanol) = 5.0, 7.5 and 10%) systems, whereas there is no percolation phenomenon in the butanol ($\nu$(butanol) = 2.5%) system. In Figure 1d, for water/AOT/IPM/pentanol systems, $\sigma$ increase initially with increasing $W_0$, and reach a maximum, followed by a slow decrease. No percolation phenomenon is observed in water/AOT/IPM/pentanol systems.

To compare the effect of added alcohol in altering the interface to induce percolation, the variation of the threshold water content ($W_p$) with alcohol content is presented in Figure S2 (Supporting Information). For water/AOT/IPM/ethanol (propanol) systems, $W_p$ decreases sharply with the increase of ethanol (propanol) content initially, then keeps almost unchanged above 7.5% ethanol (propanol) content, which indicates that ethanol (propanol) promotes the percolation. However, $W_p$ of water/AOT/IPM/butanol systems increases gradually with increasing butanol concentration, which indicates butanol retards the percolation. In addition, $W_p$ decreases as alcohol chain length reduces, which corresponds to the increase of interdroplet attractive interactions.[40] $W_p$ is closely correlated with the water solubilization capacities of


dx.doi.org/10.1021/jp210902r | J. Phys. Chem. B 2012, 116, 3723−3734

water/AOT/IPM/alcohol systems, which will be further discussed in the following part.

Here, the water solubilization capacities of water/AOT/IPM/alcohols systems at different alcohol concentrations are examined according to Figure 1 and displayed in Figure 2. The

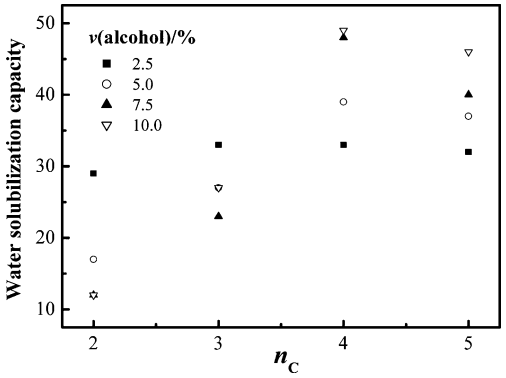


**Figure 2.** Variation of water solubilization capacity with alcohol chain length ($n_c$) in water/AOT/IPM/alcohol systems.

water solubilization capacities of water/AOT/IPM/ethanol (propanol) systems decrease with increasing alcohol concentration, whereas those of water/AOT/IPM/butanol (pentanol) systems increase. And the water solubilization capacity increases drastically from ethanol to butanol at alcohol content ≥5.0%, then decreases slightly from butanol to pentanol. Similar results have been obtained with other systems based on the surfactant AOT,[45] cationic surfactants,[46] and nonionic surfactants.[40,47−49] The water solubilization capacities of water/AOT/IPM/alcohols systems varied with alcohol chain length may be interpreted by considering the two main factors that control the growth of the droplets. The growth of droplets during the solubilization process is limited either by the radius of the spontaneous curvature of the interface, $R^o$, as the result of the curvature effect or by the critical radius of droplet, $R^c$, due to the attractive interactions among droplets.[45,46] These two radii depend in opposite ways on variables which determine the water solubilization such as $N_S$, $N_A$, and $N_O$ (where $N_S$, $N_A$, and ,$N_O$ are the chain lengths of surfactant, alcohol, and oil, respectively), surfactant headgroup size, etc.[48,49] Thus, the solubilization capacity is dependent on the influence of alcohols on the spontaneous curvature and the interdroplets attractive interactions. For the water/AOT/IPM/pentanol system dominated by $R^o$, the water solubilization capacity is inversely proportional to the lateral pressure exerted by the alcohol at the hydrophobic part of the interface. In contrast, for the water/AOT/IPM/ethanol (propanol, butanol) systems dominated by $R^c$, the water solubilization capacities are inversely proportional to the interdroplet attractive interactions,[46,50] and the interactions are directly related to the thickness of the penetrable interfacial layer $N_S-N_A$. Thus, $R^c$ and water solubilization capacity increase with $N_A$, and the percolation phenomenon is associated with the water solubilization capacity.[51] An increase in the attractive interactions between droplets produces an increase of the lifetime of two or more associated droplets, which facilitates the migration of the counterions of the surfactant from one droplet to another and leads to the percolation. Therefore, the interdroplet attractive interactions decrease as alcohol chain length increases, corresponding to the water solubilization capacity and $W_p$ increase, and even no percolation in the pentanol system.

It is interesting to observe that $\sigma$ decreases gradually in the sequence of ethanol, propanol, butanol, and pentanol at the same alcohol concentration and $W_0$. Similar phenomenon has been also observed by Suarez et al.[51] in water/AOT/decane/alcohol and Li et al.[52] in water/TX-100/heptane/alcohol systems. The conductance behaviors of water/AOT/IPM/alcohol systems are closely correlated with the physical properties of alcohol such as polarity, viscosity, and hydrophilicity. Table 1 lists the physical properties of alcohols and

**Table 1. Physical Properties of Alcohols and IPM**

| solvents | viscosity (mPa·S) (30 °C) | dielectric const (20 °C) |
|---|---|---|
| ethanol | 0.991 | 25.3 |
| propanol | 1.722 | 20.8 |
| butanol | 2.948[a] | 17.8 |
| pentanol | 3.560 | 16.9 |
| IPM | 4.280 | – |

[a]Data at 20 °C. Viscosities of pentanol and IPM are measured at the shear rate of 3000 $S^{-1}$, and the other viscosities are taken from *Langer's Handbook of Chemistry*, 15th ed.; 1998). Dielectric constants are also taken from *Langer's Handbook of Chemistry*.

**Table 2. Viscosities of Mixed Solvents at 30°C**

| | viscosity[a] of mixed solvents (mPa·S) | | | |
|---|---|---|---|---|
| alcohol vol fraction/(%) | IPM/ethanol | IPM/propanol | IPM/butanol | IPM/pentanol |
| 2.5 | 3.96 | 4.03 | 4.05 | 4.16 |
| 5.0 | 3.76 | 3.91 | 3.96 | 4.13 |
| 7.5 | 3.59 | 3.75 | 3.83 | 4.05 |
| 10.0 | 3.45 | 3.62 | 3.71 | 3.89 |

[a]Viscosities are measured at the shear rate of 3000 $S^{-1}$.

IPM and Table 2 the viscosities of mixed solvents. The dielectric constant of alcohol decreases gradually with increasing alcohol chain length, indicating the decrease of polarity. This suggests that ethanol, propanol, and butanol with the larger dielectric constant are fair mediums for ionic conduction, which facilitates the process of ionic conductance. However, pentanol with the lower dielectric constant is not a good medium, and is disadvantageous to ionic conduction. In addition, viscosity is also an important factor in influencing the conductance behavior. When the solvent with high viscosity acts as the oil phase of the microemulsion, it will prevent the droplets from colliding and aggregating into clusters, which is not benefical to the percolation occurrence.[30] The viscosity of pure alcohol increases with increasing alkyl chain length and that of mixed solvents decreases gradually with the increase of alcohol concentration. In ethanol systems, the viscosity of mixed solvents decreases markedly with the increase of ethanol concentration, which is greatly helpful to collision and fusion of droplets. In propanol (butanol) systems, the viscosities are higher than that of ethanol and IPM mixture at the same alcohol concentration, which is not beneficial to the collision and fusion of droplets. In the pentanol system, the viscosity is the highest among the mixed solvents studied, which restrains the droplets from colliding and fusing.


dx.doi.org/10.1021/jp210902r | J. Phys. Chem. B 2012, 116, 3723−3734

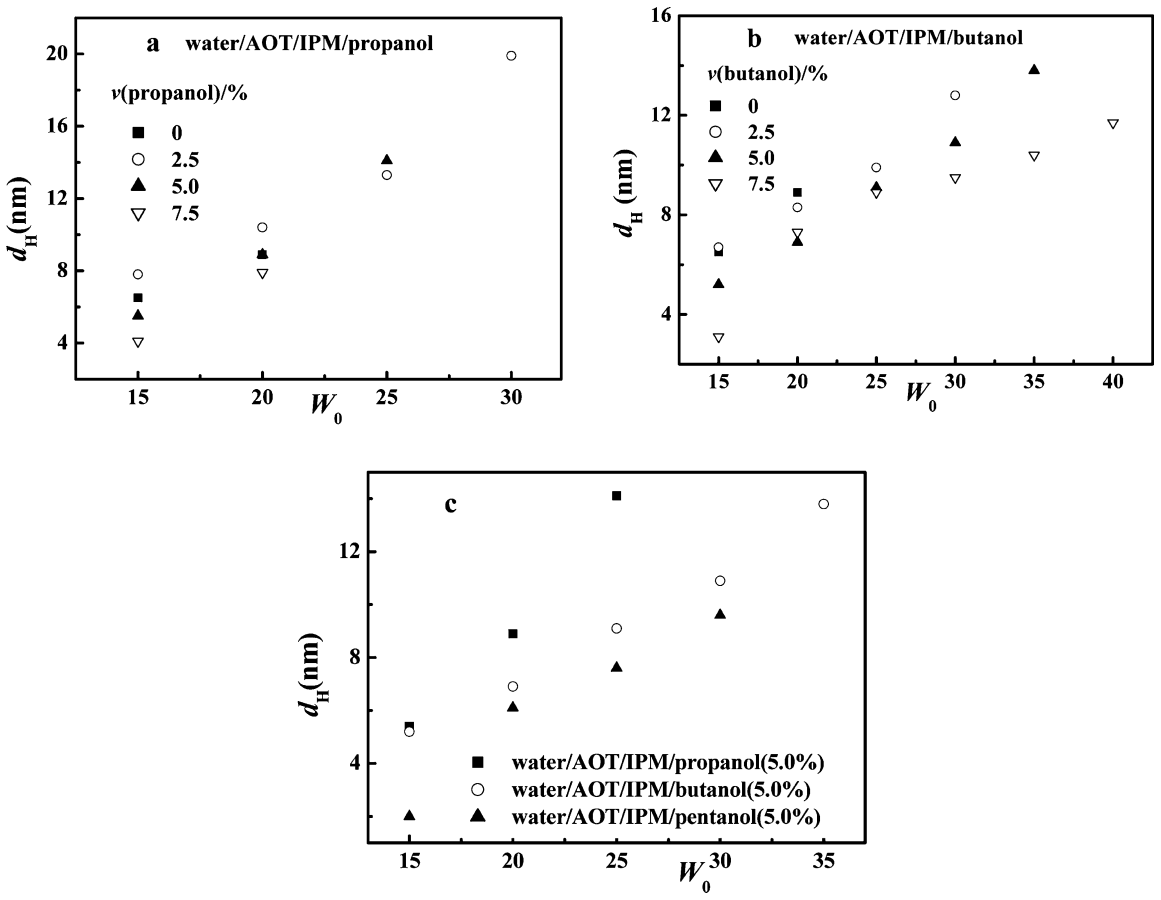


**Figure 3.** Dependence of $d_H$ on $W_0$ in water/AOT/IPM/alcohol systems.

Ethanol, propanol, and butanol, but not pentanol, induce distinctly the percolation occurrence, which may be explained by the interfacial flexibility and the attractive interactions between droplets. Conductance formation of an AOT-based microemulsion is mainly due to the transfer of $Na^+$ ions through the transient channels formed between colloiding droplets.[53,54] The interfacial flexibility and the attractive interactions between droplets determine the exchange rates of $Na^+$ ions and water molecules,[6] which play the dominant role in the droplets collision and fusion process. The micelles usually possess three solubilization sites: the oil phase, the micellar interface, and the intramicellar waterpool.[55] Ethanol is mainly located in the micellar waterpool and interacts with AOT in the interior micelle interface,[56,57] Though the interaction is similar to that of glycerol (ethylene glycol) and AOT,[11] the former is much weaker than the latter, which makes droplets grow up slightly with increasing ethanol concentration.[57,58] Meantime, the solubilization of ethanol in the waterpool can decrease the association interaction between water molecules and headgroups of AOT by weakening the polarity of water, which results in decrease of interfacial rigidity of droplets and benefits the formation of transient channels between the consecutive droplets.[52] Moreover, the interdroplet attractive interactions become stronger with increasing alcohol concentration,[58] and the droplets become more interconnected and form easily the transient channel for $Na^+$ ions transfer with increasing water content, and thus conductivity enhances sharply with the increase of water content and ethanol concentration, and the percolation occurs at the lower $W_0$. Propanol with the longer alkyl chain and more lipophilicity than ethanol might solubilize in the micellar waterpool and the interface layer, and the flexibility of the interfacial film and the attractive interactions between droplets increase with increasing propanol concentration, which are weaker than that of ethanol system at the same alcohol concentration. Thus, $W_p$ decreases gradually, but yet it is higher than that of ethanol system at the same alcohol concentration. The hydrophobic butanol may distribute preferentially at the interfacial layer. In butanol systems, the low water solubilization capacity at low butanol concentration makes the percolation phenomenon difficult to be observed. The interfacial film becomes more elastic with the increase of butanol concentration, and water solubilization capacity of the system increases apparently, which indicates that the attractive interactions between droplets decrease and are weaker than those of ethanol (propanol) systems. Thereby, the percolation phenomenon can be observed at higher $W_p$ in the butanol systems with $v$(butanol) of 5.0, 7.5, and 10.0%. In pentanol systems, the ability of alcohol molecules to penetrate into the micelle interface decreases since pentanol has longer alkyl chain than butanol; pentanol molecules may solubilize in the surfactant tail region (micellar interface) and so push the surfactant headgroups together.[28] Thus, the rigidity of interfacial film in the pentanol system should be the highest among the alcohol systems studied. In addition, the attractive interactions between droplets are very weak. Therefore, the highest rigidity of the interfacial film and the very weak interdroplet attractive interactions make the droplets' collision and fusion difficult, and thus no percolation is detected in the water/AOT/IPM/pentanol systems. The roles of the interfacial flexibility and the attracitive interactions between droplets in


dx.doi.org/10.1021/jp210902r | J. Phys. Chem. B 2012, 116, 3723−3734

the percolation process will be further discussed in the following section.

**3.2. Dimension of Droplets in Water/AOT/IPM/Alcohol Systems.** Because the droplets' aggregation behavior relates to the diffusion process, the percolation phenomenon may also be clarified by the dimension of droplets. For a certain system, the hydrodynamic diameter of droplets ($d_H$) is correlated with diffusion coefficient ($D$), viscosity of mixed solvents ($\eta$), and temperature ($T$), which is expressed by the Stokes−Einstein equation:

$$d_H = \frac{k_B T}{3\pi\eta D} \tag{4}$$

where $k_B$ denotes the Boltzmann constant. Figure 3, a and b, shows dependence of $d_H$ on $W_0$ in water/AOT/IPM/propanol and water/AOT/IPM/butanol systems, respectively. For comparison, Figure 3c exhibits the variation of $d_H$ with $W_0$ in water/AOT/IPM/propanol (butanol and pentanol) systems at the same alcohol concentration of 5.0%. The droplets of water/AOT/IPM/alcohol systems do scatter very weakly at $W_0 < 15$, and the hydrodynamic diameter is almost under 3 nm, which is below the particle size magnitude detectable with reliability by DLS.[20] Consequently, $W_0 = 15$ is selected as a measuring start point in experiments. The results show that $d_H$ of water/AOT/IPM/propanol (butanol) systems decreases with the increase of alcohol concentration. In Figure 3a, $d_H$ value of water/AOT/IPM/propanol ($v$(propanol) = 2.5%) system is larger than that of water/AOT/IPM at the same $W_0$. The similar phenomenon has been also reported in the literature.[58] $d_H$ almost increases linearly with the increase of $W_0$ in water/AOT/IPM/propanol ($v$(propanol) = 5.0, 7.5%) systems. In Figure 3b, $d_H$ has a good linear relation with $W_0$ in water/AOT/IPM/butanol ($v$(butanol) = 2.5, 5.0%) systems; however, for water/AOT/IPM/butanol ($v$(butanol) = 7.5%) system, $d_H$ increases rapidly with the increase of $W_0$ initially, then increases slowly at $W_0 > 25$. Furthermore, $d_H$ reduces in the sequence of propanol, butanol, and pentanol at the same alcohol concentration and $W_0$ in Figure 3c, which has been also found by Suarez et al.[51]

The effect of alcohol on $d_H$ may be explained by the solubilization site of alcohol. Propanol, butanol, and pentanol molecules penetrate into the micellar interface due to their small molar volumes. The smaller the molar volume of alcohol, the more are the molecules penetrating into the interface, and the greater is the difference in composition between the micellar interface and the oil phase.[12] Propanol molecules are mainly solubilized in the water pool and the micellar interface due to their solubility with water, butanol, and pentanol molecules being mainly located at the micellar interface; moreover, the amount of alcohol at the interface increases with the increase in added alcohol concentration. The total interface area becomes larger as the alcohol molecules are incorporated at the interface layer. An increase in the interface area causes the number of droplets to increase and the droplet size to shrink.[58] Thus, $d_H$ decreases gradually with the increase of alcohol concentration. In addition, the alcohol−AOT complex is formed due to an interaction between the hydroxyl group of alcohol and the headgroup of AOT.[57] This increases micelle curvature, promoting the formation of smaller micelles. For water/AOT/IPM/alcohol sytems, the difference in composition between the micellar interface and the oil phase increases as the alcohol chain shortens, which results in the increase of the interdroplet attractive interaction and droplet size. Thus, the propanol system has the largest $d_H$ at the same alcohol concentration.

The droplet sizes depend, among many other variables, on the surfactant packing parameter ($P$). For a mixed AOT/alcohol system, the effective packing parameter ($P_{eff}$) can be calculated using the relationship proposed by Ninham:[59]

$$P_{eff} = \frac{(xv/al_c)_{AOT} + (xv/al_c)_{alcohol}}{x_{AOT} + x_{alcohol}} \tag{5}$$

where $x$ are the mole fractions of the species present at the interface, $v$ and $l_c$ are the volume and the critical length of the hydrocarbon chain, respectively, and $a$ is the cross-sectional area of the surfactant headgroup. For AOT, $v/al_c > 1$; for the straight alcohol, the $v/l_c$ value is also larger than $a$, $v/al_c > 1$.[60] The addition of alcohol will reduce the average cross-sectional area of the surfactant headgroup and make $P_{eff}$ become larger, the interface curvature increases, and $d_H$ decreases. The higher the amount of alcohol in the interface layer, the smaller is $d_H$. For propanol systems, the $P_{eff}$ value may be smaller than those of butanol (pentanol) systems because some propanol molecules reside in water pool, and thus the $d_H$ of the former is larger than that of the latter. The more hydrophobic pentanol distributes in the interface layer and oil phase, and it limits the flexibility of the surfactant film; thus, $d_H$ is smallest among the alcohol systems studied.

Here, the percolation mechanism of water/AOT/IPM/alcohol systems may be rationally understood by $d_H$. For the alcohol systems, $d_H$ decreases gradually as alcohol concentration increases at the same $W_0$. The decrease in size of the droplets produces a decrease in the overlapping of the interfaces of the colliding droplets which account for the decrease of the interdroplet attractive interactions,[51] which is not benefical to droplets' collision and fusion. However, the percolation of the propanol system happens apparently at the lower $W_0$ with increasing propanol concentration. This implies that the interfacial flexibility plays a dominant role in contributing to the percolation. The enhancement of the interfacial flexibility with the increase of alcohol concentration will benefit the opening up of the interface of collision droplets, which makes droplets easy for collision and fusion. Compared to the propanol system, the butanol system has the smaller $d_H$ at the same $W_0$ and alcohol concentration, which is not very helpful to droplets' collision and fusion. However, there is larger number density of droplets in unit volume in the butanol system than that of the propanol system, which increases the probability of droplets' collision and fusion. In addition, the interfacial flexibility also increases with the increase of butanol concentration, which assists droplets' collision and fusion. Moreover, the water solubilization capacity increases gradually with the increase in butanol content as mentioned earlier, and $d_H$ grows large enough as the water content reaches $W_p$, which is helpful to droplets' collision and fusion. These result in the percolation occurrence at the higher $W_p$ in the butanol system. For the pentanol system, though $d_H$ is very close to that of the butanol system at the same $W_0$ and alcohol concentration, the interfacial rigidity of the pentanol system is the highest among the alcohol systems studied, and the high rigidity makes shape fluctuations little favorable, which makes droplets difficult to collide and fuse. Furthermore, the attractive interactions between droplets follow the increasing order of pentanol < butanol < propanol at same alcohol concentration. The strong attractive interactions between droplets will benefit droplets'

collision and fusion. These reasons result in the percolation phenomenon observed in Figure 1.

**3.3. Structure Determination of Water/AOT/IPM/Alcohol Systems.** In order to explore the influence of alcohols on the structure of water/AOT/IPM/alcohol systems, the variations of scattering intensity $I(q)$ with $q$ in water/AOT/IPM and water/AOT/IPM/butanol systems are measured and presented in Figures 4 and 5, respectively, and that of water/AOT/IPM/propanol systems is shown in Figure S3 in the Supporting Information. The scattering curves reach horizontally toward zero $q$ in the low $W_0$ range, indicating the presence of globular type particles in the systems.[22] For water/AOT/IPM and water/AOT/IPM/butanol (propanol) systems, $I(q)$ in the small $q$ region increases evidently with increasing $W_0$, and in the high $q$ region (or cross-section region) it shifts apparently toward the forward direction; in the small $q$ region it decreases with increasing alcohol concentration. Similar phenomenon has been also observed by Hirai et al.[61,62] in the water/AOT/alkane systems. These features of the scattering curves well reflect an enlargement of the micellar size with increasing $W_0$ and a decrease with increasing alcohol concentration.

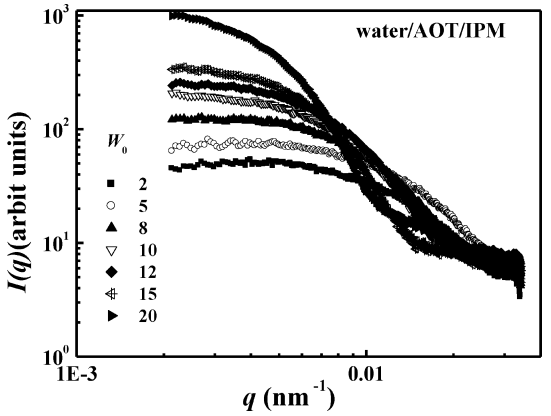


**Figure 4.** Dependence of $I(q)$ on $q$ at different $W_0$ in the water/AOT/IPM system.

The pair distance distribution function $p(r)$ is calculated according to eq 1, and the curves of $p(r)$ vs $r$ at different $W_0$ in water/AOT/IPM and water/AOT/IPM/alcohol systems are shown in Figures 6 and 7, respectively. For the water/AOT/IPM system, the curves present a slightly asymmetric bell-shaped peak accompanying a shoulder peak at $W_0$ = 2, and a low hump besides a shoulder peak at $W_0$ = 5. The shoulder peak disappears gradually with increasing $W_0$, wherein the heavy tail phenomenon presents at higher $W_0$. In addition, the well symmetric bell-shaped peaks only display at $W_0$ = 15, 20 in the curves. The bell-shaped peak shifts apparently to the higher $r$ with increasing $W_0$, indicating the growth of the micellar size, which is in good agreement with the results in Figure 4.

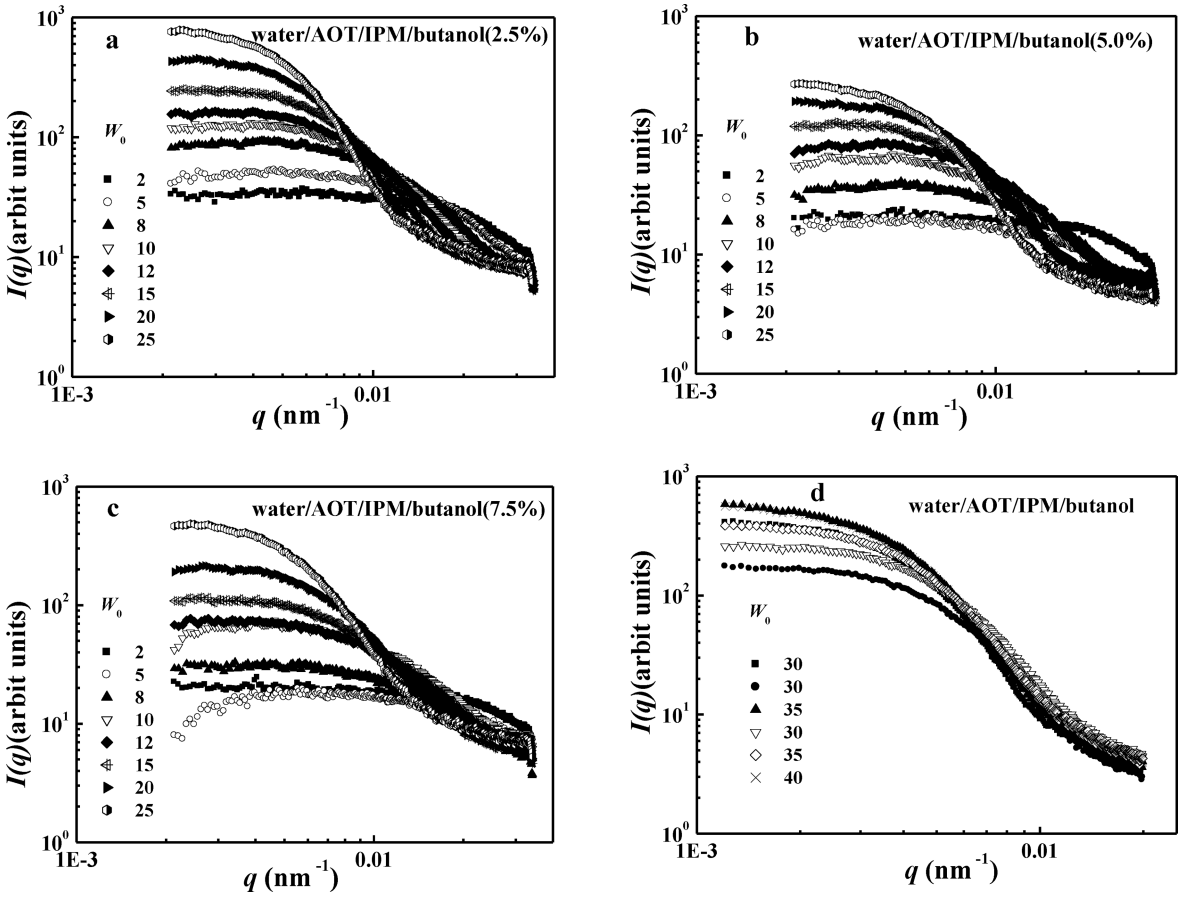


**Figure 5.** Dependence of $I(q)$ on $q$ at different $W_0$ in water/AOT/IPM/butanol systems (the sample-to-detector distance for a, b, and c was 67 cm, and that for d was 108 cm. In d, (■) water/AOT/IPM/butanol (2.5%); (●, ▲) water/AOT/IPM/butanol (5.0%); (▽, ◊, ×) water/AOT/IPM/butanol (7.5%).


dx.doi.org/10.1021/jp210902r | J. Phys. Chem. B 2012, 116, 3723−3734

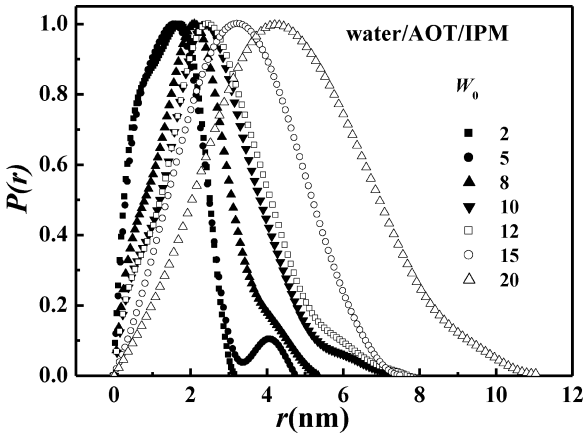


**Figure 6.** Curves of the normalized pair distance distribution function $p(r)$ vs $r$ at different $W_0$ in the water/AOT/IPM system.

Furthermore, the low hump is located at about 2.5 times the distance compared with the maximum peak in the curve. The appearance of the low hump or the shoulder peaks can be attributed to the presence of oligomeric particles such as dimer or trimer,[61,63] and the heavy tail suggests that the structure of reverse micelles is not spherical but ellipsoidal.

For water/AOT/IPM/propanol ($v$(propanol) = 2.5, 5.0, and 7.5%) systems, the shoulder peaks appear in the $W_0$ ranges of 5−15, 8−15, 10−15, and the low hump peaks appear in the $W_0$ ranges of 8−12, 10−12, 10−15, respectively. For butanol ($v$(butanol) = 2.5, 5.0, 7.5%) systems, the shoulder peaks appear in the $W_0$ ranges of 5−20, 8−20, 8−20, and the low hump peaks appear in the $W_0$ ranges of 8−12, 10−15, 10−15, respectively. For the pentanol ($v$(pentanol) = 5.0%) system, the shoulder and the low hump peaks appear in the $W_0$ ranges of 5−25 and 10−12, respectively. Compared to the water/AOT/IPM system, the shoulder and low hump peaks of water/AOT/IPM/propanol (butanol) systems begin to appear at higher $W_0$ with increasing alcohol concentration, accompanying the obvious heavy tail. This may be due to the micellar dimension reduction with increasing alcohol concentration. In addition, the low hump peaks in water/AOT/IPM/propanol ($v$(propanol) = 2.5%) system are mostly located about 2.5 times the distance compared with the maximum peaks, and those in propanol ($v$(propanol) = 5.0, 7.5%) systems transfer from 5 times to 2.5 times distance with the increase in $W_0$; however, those in water/AOT/IPM/butanol (pentanol) systems are almost located at twice distance. The maximum peak in the $p(r)$ curve can be related to very small structures like discrete droplets, and the shoulder or the low hump peak to larger structures like oligomers. This indicates that a large proportion of particles in the system is the discrete droplets and a small proportion is the oligomers. The extent of the appearance of the shoulder or the low hump peaks may reflect the ratio of oligomers to all particles in the system.

The gyration radii ($R_g$) in water/AOT/IPM and water/AOT/IPM/alcohols systems are calculated by eq 3 from the $p(r)$ plot, as shown in Figure 8. For the water/AOT/IPM system, $R_g$ increases slowly at $W_0 \leq 5$, followed by a linear increase at $W_0 > 5$. $R_g$ in water/AOT/IPM/propanol (butanol) ($v$(alcohol) = 2.5%) systems increase linearly in the $W_0$ range studied; the trends of $R_g$ changing with $W_0$ in water/AOT/IPM/propanol (butanol) ($v$(alcohol) = 5.0, 7.5%) systems are similar to that of water/AOT/IPM system. In addition, $R_g$ decrease with the increase of propanol (butanol) concentration from 2.5 to 7.5% at the same $W_0$. To further comprehend the effect of different alcohols on $R_g$, Figure 8c shows specially the dependence of $R_g$ on $W_0$ in water/AOT/IPM/propanol (butanol and pentanol) systems at an alcohol concentration of 5.0%. $R_g$ of three curves are very close at $W_0 \leq 12$. $R_g$ of water/AOT/IPM/propanol system are much higher than those of water/AOT/IPM/butanol (pentanol) systems at $W_0 > 12$. The trends of $R_g$ changing with $W_0$ are consistent with that of $d_H$ obtained from DLS. It is worthwhile to notice that the trends of $R_g$ changing with $W_0$ in water/AOT/IPM and water/AOT/IPM/alcohol systems are evidently different from those of water/AOT/alkane systems. According to the slopes of $R_g$ vs $W_0$ curves in water/AOT/alkane systems, Hirai et al.[61,62] have brought forward that the three phases (oligomeric phase, transient phase, and monomeric phase) corresponded to three $W_0$ regions, respectively. Combining Figure 7 with Figure 8, it can be deduced that the different phases that existed in water/AOT/IPM/alcohol systems correspond to the three $W_0$ ranges. At $W_0 < 5$, the discrete droplets exist in the system; lots of big droplets companying large oligomers exist at $5 \leq W_0 < 15$ for propanol systems and $5 \leq W_0 < 20$ for butanol systems, which result in the great increase of $R_g$ values;[62] the isolated ellipsoidal droplets exist at $W_0 \geq 15$ for propanol systems and $W_0 \geq 20$ for butanol systems, respectively.

In order to compare the results obtained from DLS and SAXS, Table 3 lists droplets diameter ($d$) and $d_H$ of water/AOT/IPM/butanol systems at different butanol concentrations, wherein $d$ is calculated according to the equation $d = 2Rm = 2(5/3)^{1/2}R_g$ assuming monodisperse spherical droplets. It can be found that the trends of $d$ changing with $W_0$ and butanol concentration are in good agreement with those of $d_H$, and $d$ is generally smaller than $d_H$ at the same $W_0$. The results of water/AOT/IPM/propanol systems are similar to those of water/AOT/IPM/butanol (not listed). The results obtained from DLS are larger than those of SAXS, which has been also reported in the literatures.[23,64] The discrepancy of results obtained from DLS and SAXS may result mainly from their distinct particle scattering volumes.[64] Since the hydrocarbon chains of AOT and the organic solvent have quite similar electron densities, X-ray scattering consists of water core plus the headgroup portion of AOT molecules. In addition, DLS still includes the hydrocarbon tails of AOT molecules.

**3.4. Conductance Mechanism of Water/AOT/IPM/Alcohol Systems.** Three different stages exist in $\sigma-W_0$ curves of water/AOT/IPM/alcohol systems, which is similar to that of the water/AOT/heptane system.[17,65] Li et al. have put forward that three morphologies (discrete droplets, clusters, and prolate clusters) corresponded to three stages in $\sigma-W_0$ curves.[17] Can the various phases of water/AOT/IPM/alcohol systems obtained from SAXS correspond to the different stages of $\sigma-W_0$ curves or not? The schematic diagram of conductance behavior of water/AOT/IPM/alcohol systems is primarily put forward according to the sections 3.1 and 3.3, as shown in Scheme 1. Lots of the discrete droplets exist in water/AOT/IPM/alcohol systems at $W_0 < 5$. In this $W_0$ range, a few $Na^+$ ions transfer from one droplet to another, and thus $\sigma$ increases slowly. At $5 \leq W_0 < 15$ for propanol systems ($5 \leq W_0 < 20$ for butanol systems), the droplets grow up with increasing $W_0$, corresponding to the oligomers coming into being. The amount of droplets decreases gradually with droplets' growth, and the amount of oligomers increases initially and reduces gradually. As a result, lots of big droplets and oligomers


dx.doi.org/10.1021/jp210902r | J. Phys. Chem. B 2012, 116, 3723−3734

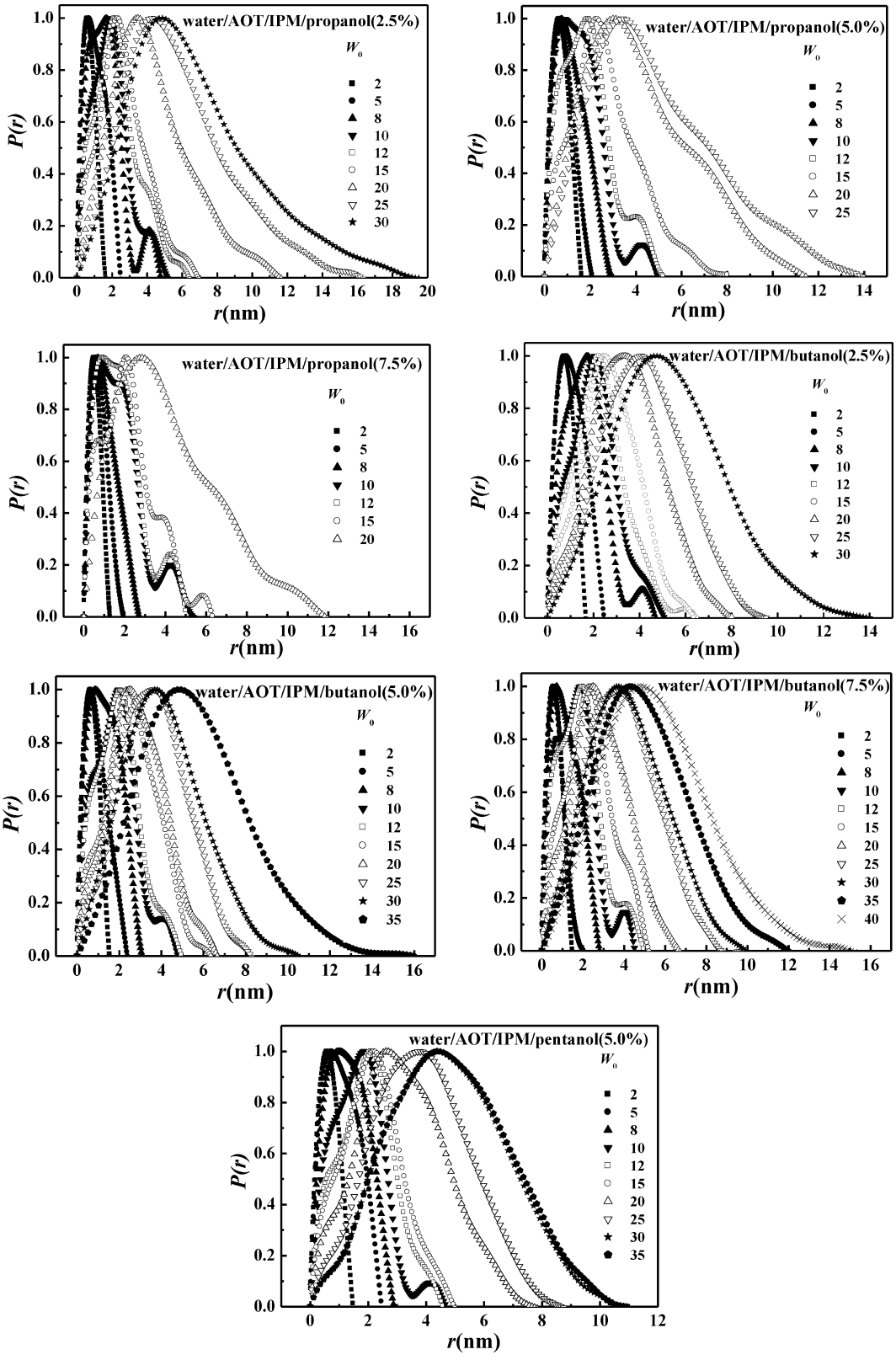


**Figure 7.** Curves of the normalized pair distance function $p(r)$ vs $r$ at different $W_0$ in water/AOT/IPM/alcohol systems.

together exist in this stage, and there is a dynamic equilibrium between them. In this $W_0$ range, a great deal of $Na^+$ ions transfer rapidly between big droplets and/or oligomers, and therefore $\sigma$ increases sharply until the maximum and then remains unchanged. At $W_0 \geq 15$ for propanol systems ($W_0 \geq 20$ for butanol systems), droplets' size continues to increase with increasing $W_0$, the amount of droplets continues to decrease, and the oligomers disappear. Moreover, the droplets change from sphericity to ellipsoid, and the isolated ellipsoidal droplets are the main form of droplets existing in the system. In


dx.doi.org/10.1021/jp210902r | J. Phys. Chem. B 2012, 116, 3723–3734

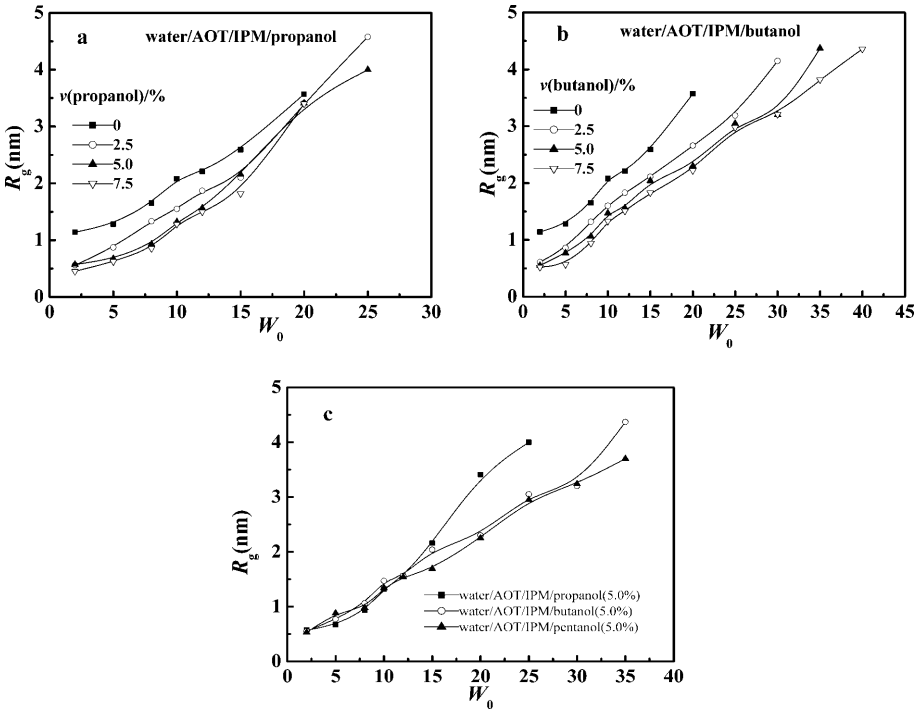


**Figure 8.** Dependence of $R_g$ on $W_0$ in water/AOT/IPM/alcohol systems.

**Table 3. Droplet Sizes of Water/AOT/IPM/Butanol Systems Measured by SAXS and DLS at Different Alcohol Volume Fractions**

| | droplet sizes by SAXS | | | | | | droplet sizes by DLS | | |
|---|---|---|---|---|---|---|---|---|---|
| | 2.5% | | 5.0% | | 7.5% | | 2.5% | 5.0% | 7.5% |
| $W_0$ | $R_g$/nm | $d$/nm | $R_g$/nm | $d$/nm | $R_g$/nm | $d$/nm | $d_H$/nm | $d_H$/nm | $d_H$/nm |
| 2 | 0.61 | 1.58 | 0.55 | 1.42 | 0.52 | 1.34 | | | |
| 5 | 0.86 | 2.22 | 0.77 | 1.99 | 0.57 | 1.47 | | | |
| 8 | 1.32 | 3.41 | 1.06 | 2.74 | 0.94 | 2.43 | | | |
| 10 | 1.60 | 4.13 | 1.47 | 3.79 | 1.33 | 3.43 | | | |
| 12 | 1.83 | 4.73 | 1.56 | 4.03 | 1.51 | 3.90 | | | |
| 15 | 2.11 | 5.45 | 2.04 | 5.27 | 1.83 | 4.73 | 6.7 | 5.2 | 3.1 |
| 20 | 2.66 | 6.87 | 2.30 | 5.94 | 2.22 | 5.73 | 8.3 | 6.9 | 7.3 |
| 25 | 3.19 | 8.24 | 3.05 | 7.88 | 2.98 | 7.69 | 9.9 | 9.1 | 8.9 |
| 30 | 4.15 | 10.72 | 3.20 | 8.26 | 3.21 | 8.29 | 12.8 | 10.9 | 9.5 |
| 35 | | | 4.37 | 11.28 | 3.82 | 9.86 | | 13.8 | 10.4 |
| 40 | | | | | 4.36 | 11.26 | | | 11.7 |

this stage, a great deal of $Na^+$ ions transfer slowly between ellipsoidal droplets, and $\sigma$ keeps unchanged or increases slowly until percolation occurrence. It is worthwhile to point out specially that nonclustered ellipsoidal droplets play the important role in the percolation process, and the similar phenomenon has been evidenced by Jahn et al. using TEM measurments.[66] The droplet structure obtained from SAXS associated with conductivity behavior will benefit us to understand well the conductivity mechanism of water/AOT/IPM/alcohol systems.

## 4. CONCLUSIONS

In this work, the structure of water/AOT/IPM/alcohol systems has been investigated systematically to thoroughly understand the percolation mechanism of reverse micelles, using conductivity, DLS, and SAXS techniques. The water-content-induced percolation is detected in water/AOT/IPM/ethanol (propanol and butanol) systems. The $W_p$ shifts evidently toward the lower value as ethanol (propanol) content increases from 2.5 to 10.0%, and the opposite is observed for butanol. The percolation phenomenon is discussed from physical properties of alcohols, the interfacial flexibility, and the interdroplet attractive interactions. The interfacial flexibility increases with the reduction of alcohol chain length and the increase of alcohol concentration, and the attractive interactions between droplets increase with the reduction of alcohol chain length.

The $d_H$ increases apparently with increasing water content, while it decreases gradually with increasing alcohol concentration and its chain length. The variation of $d_H$ with alcohol type and its concentration may be rationally understood by the solubilization site of alcohol and packing parameter ($P$). The percolation mechanism of water/AOT/IPM/alcohol systems is further analyzed by $d_H$. It confirms that the interfacial flexibility and the attractive interactions between droplets play the dominant role in the percolation process.


dx.doi.org/10.1021/jp210902r | J. Phys. Chem. B 2012, 116, 3723−3734

**Scheme 1. Schematic Diagram of Conductance Behavior of Water/AOT/IPM/Alcohol Systems**

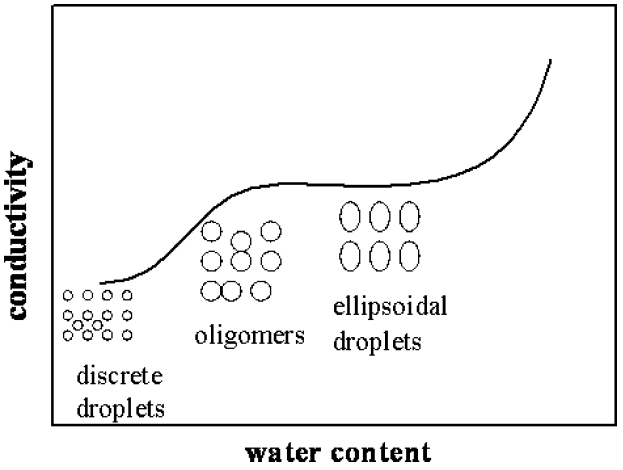


The shoulder and the low hump peaks are present with the increase of $W_0$ in $p(r)$ profile, indicating the existence of oligomers in the system, which depends on alcohol type and concentration. $R_g$ almost increases linearly with increasing $W_0$, and decreases with the increase of alcohol chain length and concentration. The trends of $d$ changing with $W_0$ and alcohol concentration are consistent with those of $d_H$, and $d$ is generally smaller than $d_H$ at the same $W_0$. Conductance mechanism of water/AOT/IPM/alcohol systems is primarily put forward in this study. The three phases (discrete droplets, oligomers, and isolated ellipsoidal droplets) in water/AOT/IPM/alcohol systems correspond to the different stages in $\sigma-W_0$ curves.

## ■ ASSOCIATED CONTENT

### Supporting Information

Dependence of $\sigma$ on $W_0$ in the water/AOT/IPM system (Figure S1). Variation of the threshold water content ($W_p$) with alcohol content in water/AOT/IPM/alcohol systems (Figure S2). Dependence of $I(q)$ on $q$ at different $W_0$ in water/AOT/IPM/propanol systems (Figure S3). This material is available free of charge via the Internet at http://pubs.acs.org.

## ■ AUTHOR INFORMATION

### Corresponding Author

*Fax: +86-22-23505948. E-mail: xgzhang@nankai.edu.cn (X.G.Z.); jxliu@hebut.edu.cn (J.X.L.).

### Notes

The authors declare no competing financial interest.

## ■ ACKNOWLEDGMENTS

The authors are grateful for the financial support by the Natural Science Foundation of Tianjin, China (08JCYBJC00700), and Natural Science Foundation of Hebei province, China (B2011202118).

## ■ REFERENCES

(1) Zhou, G. W.; Li, G. Z.; Chen, W. J. *Langmuir* **2002**, *18*, 4566–4571.
(2) Correa, N. M.; Pires, P. A. R.; Silber, J. J.; Seoud, O.A. E. *J. Phys. Chem. B* **2005**, *109*, 21209–21219.
(3) Fanun, M. *J. Mol. Liq.* **2007**, *135*, 5–13.
(4) Abuin, E.; Lissi, E.; Cerón, A.; Rubio, M. A. *J. Colloid Interface Sci.* **2003**, *258*, 363–366.
(5) Liu, D. J.; Ma, J. M.; Cheng, H. M.; Zhao, Z. G. *Colloids Surf. A* **1998**, *139*, 21–26.
(6) Li, Q.; Li, T.; Wu, J. G. *J. Colloid Interface Sci.* **2001**, *239*, 522–527.
(7) Hait, S. K.; Sanyal, A.; Moulik, S. P. *J. Phys. Chem. B* **2002**, *106*, 12642–12650.
(8) Mukhopadhyay, L.; Mitra, N.; Bhattacharya, P. K.; Moulik, S. P. *J. Colloid Interface Sci.* **1997**, *186*, 1–8.
(9) Goto, A.; Harada, S.; Fujita, T.; Niera, Y.; Yoshioka, H.; Kishimoto, H. *Langmuir* **1993**, *9*, 86–89.
(10) Vasquez, V. R.; Williams, B. C.; Graeve, O. A. *J. Phys. Chem. B* **2011**, *115*, 2979–2987.
(11) Falcone, R. D.; Silber, J. J.; Correa, N. M. *Phys. Chem. Chem. Phys.* **2009**, *11*, 11096–11100.
(12) Agazzi, F. M.; Falcone, R. D.; Silber, J. J.; Correa, N. M. *J. Phys. Chem. B* **2011**, *115*, 12076–12084.
(13) Tomšič, M.; Podlogar, F.; Gašperlin, M.; Bešter-Rogač, M.; Jamnik, A. *Int. J. Pharm.* **2006**, *327*, 170–177.
(14) Feitosa, E.; Cavalcante, V. R. O.; Amaral, L. Q. *Colloids Surf. A* **2009**, *348*, 82–86.
(15) Müller, M.; Süthn, B.; Busse, K.; Kressler., J. *J. Colloid Interface Sci.* **2009**, *335*, 228–233.
(16) Hait, S. K.; Moulik, S. P.; Rodgers, M. P.; Burke, S. E.; Palepu, R. *J. Phys. Chem. B* **2001**, *105*, 7145–7154.
(17) Li, Q.; Li, T.; Wu, J. G. *J. Phys. Chem. B* **2000**, *104*, 9011–9016.
(18) Maitra, A. N.; Mathew, C.; Varshney, M. *J. Phys. Chem.* **1990**, *94*, 5290–5292.
(19) Jada, A.; Lang, J.; Zana, R. *J. Phys. Chem.* **1989**, *93*, 10–12.
(20) Mendonça, C. R. B.; Silva, Y. P.; Böckel, W. J.; Simó-Alfonso, E. F.; Ramis-Ramos, G.; Piatnicki, C. M. S.; Bica, C. I. D. *J. Colloid Interface Sci.* **2009**, *337*, 579–585.
(21) Tomšič, M.; Bešter-Rogač, M.; Jamnik, A.; Kunz, W.; Touraud, D.; Bergmann, A.; Glatter, O. *J. Colloid Interface Sci.* **2006**, *294*, 194–211.
(22) Shrestha, L. K.; Dulle, M.; Glatter, O.; Aramaki, K. *Langmuir* **2010**, *26*, 7015–7024.
(23) Blochowicz, T.; Gögelein, C.; Spehr, T.; Müller, M.; Stühn, B. *Phys. Rev. E* **2007**, *76*, 041505.
(24) Liu, D. J.; Ma, J. M.; Cheng, H. M.; Zhao, Z. G. *Colloids Surf. A* **1998**, *143*, 59–68.
(25) Moulik, S. P.; De, G. C.; Bhowmik, B. B.; Panda, A. K. *J. Phys. Chem. B* **1999**, *103*, 7122–7129.
(26) Ray, S.; Bisal, S. R.; Moulik, S. P. *J. Chem. Soc., Faraday Trans.* **1993**, *89*, 3277–3282.
(27) Ray, S.; Paul, S.; Moulik, S. P. *J. Colloid Interface Sci.* **1996**, *183*, 6–12.
(28) Nazzario, L. M. M.; Hatton, T. A.; Crespo, J. P. S. G. *Langmuir* **1996**, *12*, 6326–6335.
(29) Mukhopadhyay, L.; Bhattcharya, P. K.; Moulik, S. P. *Colloids Surf.* **1990**, *50*, 295–308.
(30) Liu, D. J.; Ma, J. M.; Cheng, H. M.; Zhao, Z. G. *J. Dispersion Sci. Technol.* **1999**, *20*, 513–533.
(31) von Corswant, C.; Söderman, O. *Langmuir* **1998**, *14*, 3506–3511.
(32) Attwood, D. In *Colloid Drug Delivery System*; Kreuter, J., Ed.; Marcel Dekker Inc.: New York, 1994; p 31.
(33) Paul, B. K.; Mitra, R. K. *J. Colloid Interface Sci.* **2005**, *288*, 261–279.
(34) Mitra, R. K.; Paul, B. K. *Colloids Surf. A* **2005**, *252*, 165–180.
(35) Paul, B. K.; Mitra, R. K. *J. Colloid Interface Sci.* **2006**, *295*, 230–242.
(36) Mitra, R. K.; Paul, B. K. *Colloids Surf. A* **2005**, *252*, 243–259.
(37) Zielińska, K.; Wilk, K. A.; Jezierski, A.; Jesionowski, T. *J. Colloid Interface Sci.* **2008**, *321*, 408–417.
(38) De, M.; Bhattacharya, S. C.; Panda, A. K.; Moulik, S. P. *J. Dispersion Sci. Technol.* **2009**, *30*, 277–288.
(39) De, M.; Bhattacharya, S. C.; Moulik, S. P.; Panda, A. K. *J. Surfactants Deterg.* **2010**, *13*, 475–484.

(40) Mehta, S. K.; Kaur, G.; Mutneja, R.; Bhasin, K. K. *J. Colloid Interface Sci.* **2009**, *338*, 542−549.
(41) Wang, F.; Fang, B.; Zhang, Z.; Zhang, S.; Chen, Y. *Fuel* **2008**, *87*, 2517−2522.
(42) Moulik, S. P.; Digout, L. G.; Aylward, W. M.; Palepu, R. *Langmuir* **2000**, *16*, 3101−3106.
(43) Hait, S. K.; Moulik, S. P. *Langmuir* **2002**, *18*, 6736−6744.
(44) Glatter, O. Small angle scattering and light scattering. In *Neutron, X-ray and light scattering*; Linder, P., Zemb, Th., Eds.; Elsevier Science: New York, 1991; pp 33−60.
(45) Hou, M. J.; Shah, D. O. *Langmuir* **1987**, *3*, 1086−1096.
(46) Lang, J.; Lalem, N.; Zana, R. *J. Phys. Chem.* **1991**, *95*, 9533−9541.
(47) Yaghmur, A.; Aserin, A.; Garti, N. *Colloids Surf. A* **2002**, *209*, 71−81.
(48) Garti, N.; Aserin, A.; Ezrahi, S.; Tuval, E. *J. Colloid Interface Sci.* **1995**, *169*, 428−436.
(49) Ezrahi, S.; Tuval, E.; Aserin, A.; Garti, N. *J. Colloid Interface Sci.* **2005**, *291*, 273−281.
(50) Leung, R.; Shah, D. O. *J. Colloid Interface Sci.* **1987**, *120*, 320−329.
(51) Suarez, M. J.; Lévy, H.; Lang, J. *J. Phys. Chem.* **1993**, *97*, 9808−9816.
(52) Li, X. C.; He, G. H.; Zheng, W. J.; Xiao, G. K. *Colloids Surf. A* **2010**, *360*, 150−158.
(53) García-Río, L.; Hervés, P.; Leis, J. R.; Mejuto, J. C. *Langmuir* **1997**, *13*, 6083−6088.
(54) Kataoka, H.; Eguchi, T.; Masui, H.; Miyakubo, K.; Nakayama, H.; Nakamura, N. *J. Phys. Chem. B* **2003**, *107*, 12542−12548.
(55) Silber, J. J.; Biasutti, A.; Abuin, E.; Lissi, E. *Adv. Colloid Interface Sci.* **1999**, *82*, 189−252.
(56) Lissi, E. A.; Engel, D. *Langmuir* **1992**, *8*, 452−455.
(57) Perez-Casas, S.; Castillo, R.; Costas, M. *J. Phys. Chem. B* **1997**, *101*, 7043−7054.
(58) Lin, T. L.; Lin., H.; Lee, T. T. *Prog. Colloid Polym. Sci.* **1997**, *105*, p268−271.
(59) Evans, D. F.; Ninham, B. W. *J. Phys. Chem.* **1986**, *90*, 226−234.
(60) Aveyard, R.; Binks, B. P.; Mead, J. *J. Chem. Soc., Faraday Trans. 1* **1987**, *83*, 2347−2357.
(61) Hirai, M.; Kawai-Hirai, R.; Yabuki, S.; Takizawa, T.; Hirai, T.; Kobayashi, K.; Amemiya, Y.; Oya, M. *J. Phys. Chem. B* **1995**, *99*, 6652−6660.
(62) Hirai, M.; Kawai-Hirai, R.; Sanada, M.; Iwase, H.; Mitsuya, S. *J. Phys. Chem. B* **1999**, *103*, 9658−9662.
(63) Hirai, M.; Iwase, H.; Arai, S.; Takizawa, T.; Hayashi, K. *Biophys. J.* **1998**, *74*, 1380−1387.
(64) Amaral, C. L. C.; Itri, R.; Politi, M. J. *Langmuir* **1996**, *12*, 4638−4643.
(65) Liu, D. J.; Ma, J. M.; Cheng, H. M.; Zhao, Z. G. *Colloids Surf. A* **1998**, *135*, 157−164.
(66) Jahn, W.; Strey, R. *J. Phys. Chem.* **1988**, *92*, 2294−2301.